
Higher Order Massive Operator Matrix Elements and Heavy Quark Corrections to Deep-Inelastic Scattering

Summer school project by
Christian Fräßdorf

Supervisor: Prof. Dr. Johannes Blümlein

September 3, 2012

Abstract

In this report we are dealing with massive quark effects in the perturbative evaluation of deeply inelastic scattering. The renormalized one-loop gluon contributions to the massive operator matrix elements are calculated. The scalar parts of several two-loop diagrams are investigated.

Contents

1	Deeply Inelastic Scattering	3
2	Regularization and Renormalization	5
2.1	Dimensional Regularization	5
2.2	The $\overline{\text{MS}}$ scheme	5
3	Massive Operator Matrix Elements	5
3.1	One-Loop Diagrams	6
3.1.1	Vacuum Polarization Diagram	6
3.1.2	Line Insertion Diagram	8
3.1.3	Vertex Insertion Diagram	8
3.1.4	Renormalization of \hat{A}_{Qg}	10
3.2	Two-Loop Diagrams	10
3.2.1	First loop-topology	10
3.2.2	A Second loop-topology	12
4	Summary	14

1 Deeply Inelastic Scattering

One of the cleanest possibilities for the investigation of the structure of nucleons at short distances are experiments of high energy lepton-scattering off hadrons. The momentum transfers $|q^2|$ are usually larger than 4GeV^2 . The targets are destroyed during the interaction, hence this process is called inelastic. With the introduction of the quark model by Gell-Mann [1] and Zweig [2] the spectrum of the experimentally observed hadrons could be explained. According to this model hadrons are bound states of quarks and gluons, the latter being the particles mediating the strong interaction. The dynamic theory of these constituents is quantum chromodynamics (QCD). Deeply inelastic scattering (DIS) has played an important role in establishing QCD as an asymptotically free quantum field theory. Asymptotically free means that at very high energies the constituents of hadrons are behaving as if there were free particles.

Since the strong interaction is several orders of magnitude larger in strength than electroweak interactions it is sufficient to work at tree level in electroweak theory, see Fig. 1. The momenta

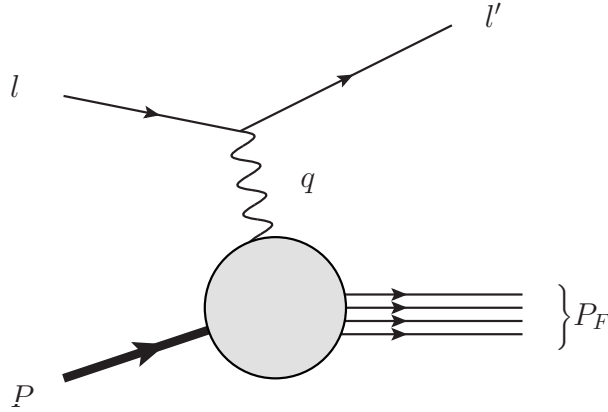


Figure 1: Feynman diagram for DIS in tree-level approximation.

of the incoming lepton and nucleon are denoted by l and P , respectively. They interact via the exchange of a virtual electroweak vector boson of momentum q . After the interaction the momentum of the scattered lepton is l' and the outgoing hadronic jet is denoted by F , carrying the total momentum P_F . Since the virtual vector boson is space-like one defines the virtuality

$$Q^2 = -q^2. \quad (1.1)$$

The process of DIS is conveniently described by using the scaling variable Bjorken- x and the variable y

$$x = \frac{Q^2}{2P \cdot q}, \quad (1.2)$$

$$y = \frac{P \cdot q}{P \cdot l}, \quad (1.3)$$

with the mass M of the nucleon, neglecting the masses of the leptons. The exchanged virtual vector boson can be, according to electroweak theory, a photon, a Z^0 - or W^\pm -boson. We restrict ourselves to electron-proton scattering. If the virtualities are not too large, i.e. $Q^2 \leq 500\text{GeV}^2$ the exchange of a Z -boson can be neglected [3]. A straightforward calculation yields the differential inclusive cross section [4]

$$l'_0 \frac{d\sigma}{d^3l'} = \frac{1}{4P \cdot l} \frac{\alpha^2}{Q^4} L_{\mu\nu} W^{\mu\nu}. \quad (1.4)$$

One observes that it factorizes into a leptonic $L_{\mu\nu}$ and a hadronic tensor $W_{\mu\nu}$. The former is well known from QED. We will concentrate on the latter object. The hadronic tensor describes the nucleon structure and is a non-perturbative quantity.

A general ansatz, taking into account its symmetry and gauge invariance, yields the expression [4]

$$W_{\mu\nu} = \frac{1}{2x} \left(g_{\mu\nu} - \frac{q_\mu q_\nu}{q^2} \right) F_L(x, Q^2) + \frac{2x}{Q^2} \left(P_\mu P_\nu + \frac{q_\mu P_\nu + q_\nu P_\mu}{2x} - \frac{Q^2}{4x^2} g_{\mu\nu} \right) F_2(x, Q^2). \quad (1.5)$$

The dimensionless functions F_L and F_2 , called structure functions, describe the composition of the nucleons. Solving (1.5) for the structure functions yields

$$F_L(x, Q^2) = \frac{8x^3}{Q^2} P^\mu P^\nu W_{\mu\nu}(q, P) \quad (1.6)$$

$$F_2(x, Q^2) = \frac{2x}{D-2} \left[(D-1) \frac{4x^2}{Q^2} P^\mu P^\nu W_{\mu\nu}(q, P) - g^{\mu\nu} W_{\mu\nu}(q, P) \right]. \quad (1.7)$$

Here, D is the dimension of space-time. With the decomposition of the hadronic tensor one obtains the expression for the differential cross section in terms of the structure functions [4]

$$\frac{d\sigma}{dx dy} = \frac{2\pi\alpha^2}{xyQ^2} \left\{ [1 + (1-y)^2] F_2(x, Q^2) - y^2 F_L(x, Q^2) \right\}. \quad (1.8)$$

Measuring the differential cross section means measuring the structure functions which in turn sheds light on the constitution of the nucleons and the nature of the strong interaction.

At large virtualities Q^2 the structure functions factorize in Mellin convolutions between the Wilson coefficients $C_i^j(x, Q^2)$ and the parton distribution functions (PDFs) $f_j(x, \mu^2)$

$$F_i(x, Q^2) = \sum_j C_i^j(x, Q^2) \otimes f_j(x, \mu^2), \quad i = 2, L, \quad (1.9)$$

which is expressed by the factorization theorem [5]. The sum over j runs over all the partons in the nucleon. The PDFs form the non-perturbative part of the structure functions, whereas the Wilson coefficients are perturbatively calculable. Here, the Mellin convolution between two functions is defined as [6]

$$[f \otimes g](x) = \int_0^1 dy \int_0^1 dz f(y) g(z) \delta(x - yz). \quad (1.10)$$

In order to reduce the number of integrals simplifying the calculations one introduces the Mellin transform [6]

$$\hat{f}(N) = \int_0^1 dx x^{N-1} f(x), \quad (1.11)$$

with N denoting the Mellin-moment, leading to a decomposition of the Mellin convolution into a product of the two Mellin transformed functions

$$\mathbf{M}[f \otimes g](N) = \mathbf{M}[f](N) \mathbf{M}[g](N). \quad (1.12)$$

This simplification will be useful later in the evaluation of the integrals occurring in massive operator matrix elements, accordingly we will work from now on in Mellin-space. In the latter, Eq. (1.9) reads

$$F_i(N, Q^2) = \sum_j C_i^j(N, Q^2) f_j(N, \mu^2). \quad (1.13)$$

2 Regularization and Renormalization

2.1 Dimensional Regularization

The loop integrals we consider are divergent in $D = 4$ dimensions. However, the divergence of a loop integral does depend on the space-time dimension. In dimensions $D \neq 4$ the corresponding momentum integrals converge, so that a natural way to regularize these infinities is to analytically continue the space-time dimension to general values for D . This procedure is known as dimensional regularization [7–10]. In this way Lorentz-invariance in Minkowski-space and other important properties of gauge field theories as for instance gauge invariance and Ward-Takahashi identities are preserved [8]. The prototype of these D -dimensional momentum integrals is given by [11]

$$\int \frac{d^D k}{(2\pi)^D} \frac{(k^2)^r}{(k^2 + R^2)^m} = \frac{\Gamma(r + D/2)\Gamma(m - r - D/2)}{(4\pi)^{D/2}\Gamma(D/2)\Gamma(m)} (R^2)^{-m+r+D/2}, \quad (2.1)$$

where k is a Euclidean 4-vector, R a scalar not depending on k and r and m integers. The verification of this equality is straightforward. The Γ -function is an analytic function in the complex plane with poles at non-positive integers. Thus, the right hand side of Eq. (2.1) can be analytically continued to arbitrary complex values for $D \neq 0, -1, -2, \dots$. We set $D = 4 + \varepsilon$ and treat ε to be an infinitesimal. Since the outcome of the loop integral is an analytic function in ε we can expand it in a Laurent series around $\varepsilon = 0$. The possible divergencies of these momentum integrals manifest themselves as poles in ε .

Furthermore, the coupling constant g has to be analytically continued. In this way the coupling acquires a mass dimension and an arbitrary scale μ has to be introduced via the substitution $g^2 \rightarrow g^2(\mu^2)^{-\varepsilon/2}$. For convenience one may introduce

$$a_s = \frac{g^2}{(4\pi)^2}, \quad (2.2)$$

after this substitution has been performed.

2.2 The $\overline{\text{MS}}$ scheme

In order to consistently remove the singularities from the theory, one has to choose a distinct renormalization scheme. A widely used scheme is the $\overline{\text{MS}}$ -scheme [12], which we will adopt below. It turns out that $1/\varepsilon$ poles always appear in the combination with one factor per loop

$$S_\varepsilon = \exp \left\{ \frac{1}{2}\varepsilon(\gamma_E - \ln(4\pi)) \right\}, \quad (2.3)$$

where γ_E is the Euler-Mascheroni constant.

In contrast to the MS-scheme [13], where only the poles in ε are subtracted, in the $\overline{\text{MS}}$ -scheme the poles are subtracted in the form $S_\varepsilon/\varepsilon$ and S_ε is set to one at the end of the calculation. As a consequence, no terms containing γ_E appear in the renormalized result which simplifies the expressions.

3 Massive Operator Matrix Elements

As mentioned in Sec. 1, the structure functions, Eq. (1.13), factorize in Mellin-space into the non-perturbative PDFs $f_j(N, \mu^2)$ and perturbatively calculable Wilson coefficients $C_i^j(x, Q^2)$. They

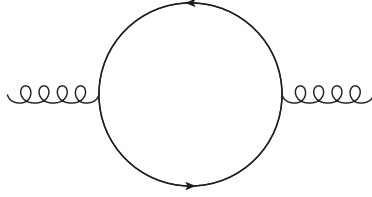


Figure 2: One-loop Vacuum polarization diagram. The curly lines denote gluons and the full lines heavy quarks.

decompose into a sum of the light $\hat{C}_i^j(N, Q^2)$ and heavy flavour Wilson coefficients $H_i^j(N, Q^2, m^2)$

$$C_i^j(N, Q^2, m^2) = \hat{C}_i^j(N, Q^2) + H_i^j(N, Q^2, m^2). \quad (3.1)$$

Furthermore, the heavy flavour part factorizes into light flavour coefficients and the massive operator matrix elements (OMEs) $A_{ij}(N, m^2)$ [14]

$$H_i^j(N, Q^2, m^2) = \sum_i \hat{C}_i^j(N, Q^2) A_{ij}(N, m^2). \quad (3.2)$$

In the following the renormalized OME A_{Qg}^r , being part of the structure function $F_2(N, Q^2)$, will be calculated up to first loop order.

3.1 One-Loop Diagrams

3.1.1 Vacuum Polarization Diagram

We first consider the one loop vacuum polarization diagram. The Feynman diagram for this process is shown in Fig. 2. The calculation of this integral corresponds to the case of $N = 1$ for an operator matrix element to be considered later. Since its evaluation requires some techniques which are indispensable for the evaluation of more complicated diagrams appearing below, we will present the calculation in detail.

The analytic expression of the amputated one-loop vacuum polarization diagram is given by

$$\Pi_{ab}^{\mu\nu}(p) = -\text{Tr} \int \frac{d^D k}{(2\pi)^D} \delta_{mj} i \frac{(\not{k} + \not{p}) + m}{(k+p)^2 - m^2} i g \gamma^\mu t_{jl}^a \delta_{ln} i \frac{\not{k} + m}{k^2 - m^2} i g \gamma^\nu t_{nm}^b. \quad (3.3)$$

Herein, m denote the quark mass and t_{ij}^a the generators of the gauge group, being $SU(3)$ for QCD, in the adjoint representation. The momentum integral consists of a numerator and a denominator, both being functions of the loop momentum k and the external momentum p . Additionally, the numerator has a Dirac-structure containing several γ -matrices. Because the vacuum polarization contains a closed Fermion-loop we have to take the trace, denoted by Tr , of these matrices simplifying the structure of the numerator. Using the relations of D -dimensional Dirac-algebra we can write

$$\text{Tr}[(\not{k} + \not{p} + m)\gamma^\mu(\not{k} + m)\gamma^\nu] = 4[(k^\mu + p^\mu)k^\nu + (k^\nu + p^\nu)k^\mu - (k+p) \cdot k g^{\mu\nu} + m^2 g^{\mu\nu}], \quad (3.4)$$

and the integral reads

$$\Pi_{ab}^{\mu\nu}(p) = -4T_f g^2 \delta_{ab} \int \frac{d^D k}{(2\pi)^D} \frac{(k^\mu + p^\mu)k^\nu + (k^\nu + p^\nu)k^\mu - (k+p) \cdot k g^{\mu\nu} + m^2 g^{\mu\nu}}{((k+p)^2 - m^2)(k^2 - m^2)}. \quad (3.5)$$

Since the representation matrices t_{ij}^a factor out they form the global color factor $T_f = 1/2$. In order to proceed, we need to combine the two denominators into a single function depending on

the scalar k^2 only. Then we make use of Eq. (2.1) and integrate the loop momentum. Further integrations over so called Feynman-parameters, needed to combine denominators, have to be carried out. The most general form of the Feynman-parameter integrals are given by [11]

$$\frac{1}{A_1^{j_1} \cdots A_n^{j_n}} = \frac{\Gamma(\sum_{i=1}^n j_i)}{\Gamma(j_1) \cdots \Gamma(j_n)} \int_0^1 dx_1 \cdots dx_n \frac{x_1^{j_1-1} \cdots x_n^{j_n-1}}{(x_1 A_1 + \cdots + x_n A_n)^{\sum_{i=1}^n j_i}} \delta\left(\sum_{i=1}^n x_i - 1\right). \quad (3.6)$$

It has to be applied to each loop integral. In the present case this relation is given by

$$\frac{1}{A^\alpha B^\beta} = \frac{\Gamma(\alpha + \beta)}{\Gamma(\alpha)\Gamma(\beta)} \int_0^1 dx \frac{x^{\alpha-1}(1-x)^{\beta-1}}{(xA + (1-x)B)^{\alpha+\beta}}, \quad (3.7)$$

leading to

$$\Pi_{ab}^{\mu\nu}(p) = -T_f g^2 \delta_{ab} \int \frac{d^D k}{(2\pi)^D} \frac{\text{Numerator}}{[(k+xp)^2 - m^2 + x(1-x)p^2]^2}. \quad (3.8)$$

Shifting the integration variable to $k' = k + xp$ and using the relations for symmetric integration [11]

$$\int \frac{d^D k}{(2\pi)^D} k^\mu f(k^2) = 0, \quad (3.9)$$

$$\int \frac{d^D k}{(2\pi)^D} k^\mu k^\nu f(k^2) = \frac{g^{\mu\nu}}{D} \int \frac{d^D k}{(2\pi)^D} k^2 f(k^2), \quad (3.10)$$

we obtain

$$\begin{aligned} \Pi_{ab}^{\mu\nu}(p) &= -T_f g^2 \delta_{ab} \int \frac{d^D k'}{(2\pi)^D} \int_0^1 dx \\ &\times \frac{8 \frac{g^{\mu\nu}}{D} k'^2 - 8x(1-x)p^\mu p^\nu - 4k'^2 g^{\mu\nu} + 4x(1-x)p^2 g^{\mu\nu} + 4m^2 g^{\mu\nu}}{[k'^2 - m^2 + x(1-x)p^2]^2}. \end{aligned} \quad (3.11)$$

Since Eq. (2.1) is only valid in a Euclidean vectorspace but the momentum four-vectors are Minkowski-space vectors we cannot apply it directly. One has to perform an analytical continuation from Minkowski- to Euclidean 4-vector-space, the Wick-rotation, since integrals can be performed only in spaces with a norm. The Wick-rotation consists of the replacements [11]

$$k^0 = i k_E^0, \quad k^2 = -k_E^2, \quad \int d^D k = i \int d^D k_E.$$

Performing this transformation we apply Eq. (2.1) and use relations for the Γ -functions to derive the following expression

$$\Pi_{ab}^{\mu\nu}(p) = 8T_f g^2 \delta_{ab} i \frac{\Gamma(2 - D/2)}{(4\pi)^{D/2}} (g^{\mu\nu} p^2 - p^\mu p^\nu) \int_0^1 dx x(1-x) [m^2 - x(1-x)p^2]^{D/2-2}. \quad (3.12)$$

Setting p on-shell, $p^2 = 0$ for massless gluons, inside the integral, it is trivial to perform the x -integration.

The final step consists in the ε -expansion. As discussed in Sec. 2 we set $D = 4 + \varepsilon$ and expand in a Laurent-series in ε and derive

$$\begin{aligned} \Pi_{ab}^{\mu\nu}(p) &= \frac{8}{3} i T_f \frac{g^2}{(4\pi)^2} \delta_{ab} (g^{\mu\nu} p^2 - p^\mu p^\nu) S_\varepsilon \left(\frac{m^2}{\mu^2}\right)^{\varepsilon/2} \frac{1}{\varepsilon} \exp\left(\sum_{n=2}^{\infty} \frac{1}{n} \left(\frac{\varepsilon}{2}\right)^n \zeta_n\right) \\ &= \frac{8}{3} i a_s T_f \delta_{ab} (g^{\mu\nu} p^2 - p^\mu p^\nu) S_\varepsilon \left(\frac{1}{\varepsilon} + \frac{1}{2} \ln\left(\frac{m^2}{\mu^2}\right) + \frac{\varepsilon}{8} \zeta_2\right). \end{aligned} \quad (3.13)$$

As expected the divergence of the integral can be described by a simple pole. The coefficient ζ_2 of the linear term in ε is the value of the Riemann ζ -function evaluated at $n = 2$.

In the next subsections we turn to the calculation of massive operator matrix elements.

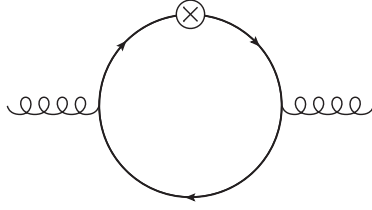


Figure 3: One-loop line insertion diagram.

3.1.2 Line Insertion Diagram

The first topology to be studied is shown in Fig. 3. It is very similar to the vacuum polarization diagram except for the fact that one of the internal propagators gets replaced by a line with an operator insertion [15–17]. This line insertion consists of two propagators and an effective vertex $\Delta(\Delta \cdot k)^{N-1}$, where Δ denotes a light-like 4-vector. The corresponding analytic expression is

$$G_{Q,ab}^{(1),\mu\nu} = -\text{Tr} \int \frac{d^D k}{(2\pi)^D} i \frac{(\not{k} - \not{p}) + m}{(k-p)^2 - m^2} \delta_{ln} i g \gamma^\mu t_{jl}^a \times i \frac{\not{k} + m}{k^2 - m^2} \Delta(\Delta \cdot k)^{N-1} i \frac{\not{k} + m}{k^2 - m^2} \delta_{mj} i g \gamma^\nu t_{nm}^b. \quad (3.14)$$

In contrast to the vacuum polarization diagram, we have to act with a projection operator onto the amputated Greens function $G_{Q,ab}^{\mu\nu}$ in order to get the OME [18]

$$A_{Qg} = \frac{1}{N_c^2 - 1} \frac{1}{D - 2} (-g_{\mu\nu}) \delta^{ab} (\Delta \cdot p)^{-N} G_{Q,ab}^{\mu\nu}. \quad (3.15)$$

In this case of external gluons the projector is merely a multiplicative constant. We apply the same strategy to solve the integral as for the vacuum polarization. The only crucial difference in its evaluation is that, due to the shift of the variable, the term $\Delta \cdot k$ becomes a binomial sum

$$(\Delta \cdot k)^N \rightarrow (\Delta \cdot k' + (1-x)\Delta \cdot p)^N = \sum_{n=0}^{N-1} \binom{N-1}{n} (1-x)^n (\Delta \cdot k')^{N-1-n} (\Delta \cdot p)^n. \quad (3.16)$$

This sum together with the residual numerator terms have to be integrated over k' . Because Δ is a light-like vector most of these terms vanish after performing the symmetric integration.

The remaining Feynman-parameter integrations take the form of Beta-functions [19]

$$B(x, y) = \int_0^1 dt t^{x-1} (1-t)^{y-1} = \frac{\Gamma(x)\Gamma(y)}{\Gamma(x+y)}, \quad \text{Re}(x), \text{Re}(y) \geq 0. \quad (3.17)$$

Having calculated all the Feynman-integrals, the ε -expansion yields the result

$$A_{Qg}^{(1)} = -8a_s T_f S_\varepsilon \left(\frac{m^2}{\mu^2} \right)^{\varepsilon/2} \frac{1}{(2+\varepsilon)\varepsilon} \exp \left(\sum_{n=2}^{\infty} \frac{1}{n} \left(\frac{\varepsilon}{2} \right)^n \zeta_n \right) \times \frac{2(N+1)(N+2) + \varepsilon(N^2 + N + 2)}{N(N+1)(N+2)} \quad (3.18)$$

3.1.3 Vertex Insertion Diagram

The second graph to be investigated is shown in Fig. 4. This diagram contains a vertex insertion,

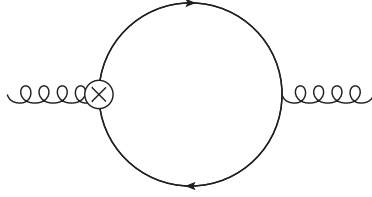


Figure 4: One-loop vertex insertion diagram.

meaning that one of the vertices is exchanged compared to the vacuum polarization diagram [15–17]. Its analytic expression reads

$$G_{Q,ab}^{(2),\mu\nu} = -\text{Tr} \int \frac{d^D k}{(2\pi)^D} i \frac{(\not{k} - \not{p}) + m}{(k-p)^2 - m^2} \delta_{ln} g t_{jl}^a \Delta^\mu \not{\Delta} \sum_{j=0}^{N-2} (\Delta \cdot (k-p))^j (\Delta \cdot k)^{N-2-j} \times i \frac{\not{k} + m}{k^2 - m^2} \delta_{mj} i g \gamma^\nu t_{nm}^b. \quad (3.19)$$

Also here the same apparatus of projecting the amputated Greens function to the OME and calculating the integral applies. The sum, stemming from the vertex insertion, can be treated exactly in the same way as in the previous diagram. Again one has to make use of the fact that Δ is a light like vector, accordingly only a few terms survive the symmetric integration. The Feynman-parameter integrals again lead to Beta-functions. Performing the ε -expansion one obtains

$$A_{Qg}^{(2)} = 32a_s T_f S_\varepsilon \left(\frac{m^2}{\mu^2} \right)^{\varepsilon/2} \frac{1}{(2+\varepsilon)\varepsilon} \exp \left(\sum_{n=2}^N \frac{1}{n} \left(\frac{\varepsilon}{2} \right)^n \zeta_n \right) \frac{1}{(N+1)(N+2)}. \quad (3.20)$$

Putting together the individual contributions from the line and vertex insertion diagrams and performing the ε -expansion to $\mathcal{O}(\varepsilon)$ one arrives at the 1-loop OME \hat{A}_{Qg}

$$\begin{aligned} \hat{A}_{Qg} &= \frac{1}{a_s} (A_{Qg}^{(1)} + A_{Qg}^{(2)}) \\ &= -T_f S_\varepsilon \left(\frac{m^2}{\mu^2} \right)^{\varepsilon/2} \frac{1}{\varepsilon} \exp \left(\sum_{n=2}^N \frac{1}{n} \left(\frac{\varepsilon}{2} \right)^n \zeta_n \right) \frac{8(N^2 + N + 2)}{N(N+1)(N+2)} \\ &= -T_f S_\varepsilon \left(\frac{m^2}{\mu^2} \right)^{\varepsilon/2} \left(\frac{1}{\varepsilon} + \frac{\zeta_2}{8\varepsilon} \right) \frac{8(N^2 + N + 2)}{N(N+1)(N+2)}. \end{aligned} \quad (3.21)$$

Here we accounted for the fact that (3.18) and (3.20) both contribute twice. In case of (3.18) the inner momentum flow has to be reversed too, giving rise to a factor $\frac{1+(-1)^N}{2}$. Introducing the leading order splitting function \hat{P}_{qg} one can write

$$\hat{A}_{Qg} = S_\varepsilon \left(\frac{m^2}{\mu^2} \right)^{\varepsilon/2} \left[-\frac{1}{\varepsilon} \hat{P}_{qg} + a_{Qg} + \varepsilon \bar{a}_{Qg} \right]. \quad (3.22)$$

and identify

$$\begin{aligned} \hat{P}_{qg} &= T_f \frac{8(N^2 + N + 2)}{N(N+1)(N+2)}, \\ a_{Qg} &= 0, \\ \bar{a}_{Qg} &= -\frac{\zeta_2}{8} \hat{P}_{qg}. \end{aligned}$$

Note that the coefficient a_{Qg} vanishes to one-loop order. Expanding Eq. (3.21) to the constant term yields the final unrenormalized $\mathcal{O}(a_s)$ OME

$$\hat{A}_{Qg} = S_\epsilon \left[-\frac{1}{\epsilon} \hat{P}_{qg} - \frac{1}{2} \ln \left(\frac{m^2}{\mu^2} \right) \hat{P}_{qg} \right]. \quad (3.23)$$

3.1.4 Renormalization of \hat{A}_{Qg}

The last step in the calculation of the OME is their renormalization. The full description of the renormalization theory of OMEs is far beyond the scope of this report, nevertheless we describe the important steps.

At $\mathcal{O}(a_s)$ coupling constant and mass renormalization do not contribute to the renormalization of \hat{A}_{Qg} , cf. [20]. There are also no collinear singularities. Thus to this order one has to add to the unrenormalized OME the inverse renormalization constant Z_{qg}^{-1} only [14], to account for the renormalization of the composite operator.

$$A_{Qg}^r = \hat{A}_{Qg} + Z_{qg}^{-1}. \quad (3.24)$$

This inverse Z -factor is given by

$$Z_{qg}^{-1} = \frac{S_\epsilon}{\epsilon} \hat{P}_{qg}. \quad (3.25)$$

The renormalized OME reads now

$$A_{Qg}^r = -\frac{1}{2} \ln \left(\frac{m^2}{\mu^2} \right) \hat{P}_{qg}. \quad (3.26)$$

At higher loop orders the renormalization of the OMEs is a complex procedure involving the calculation of the full set of renormalization constants Z_{ij} and so called transition functions Γ_{ij} , where the subscripts i, j denote the different parton types.

3.2 Two-Loop Diagrams

We will now calculate two graph-topologies at the two-loop level. In order to combine the denominators to complete squares we need to introduce more Feynman parameters which in their evaluation yield richer mathematical structures than in case of the one-loop diagrams. Since the numerator merely just increases the number of terms and thus complicating the interesting evaluation of the integrals we will neglect it here, and consider the scalar integrals only. The corresponding results indicate the principle complexity being met.

3.2.1 First loop-topology

The first diagram to be studied is given in Fig. 5 and has been studied in [14, 18]. Its analytic expression reads in the corresponding physical cases

$$I_1 = -g^4(m^2)^2 \int \frac{d^D k}{(2\pi)^D} \frac{d^D l}{(2\pi)^D} \frac{1}{(p-l)^2} \frac{1}{(l^2)^2} \frac{1}{(k-l)^2} \frac{1}{-m^2} \frac{1}{k^2 - m^2} (\Delta \cdot k)^N \frac{1}{k^2 - m^2}. \quad (3.27)$$

We integrate loop by loop with the same techniques we used in the evaluation of the one-loop diagrams, performing Wick-rotation, introducing the Feynman parametrization and perform the

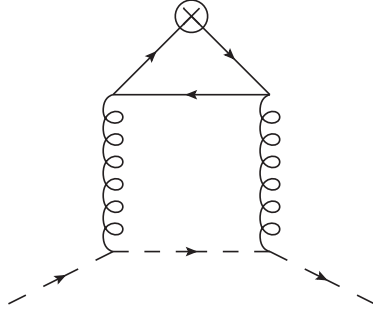


Figure 5: A pure singlet two-loop diagram. The dashed lines denote a massless quark

D -dimensional momentum integrations. After these steps, for each loop, the resulting expression for the diagram is given by

$$I_1 = \frac{\Gamma(6-D)}{(4\pi)^D} g^4 (m^2)^{-4+D} (\Delta \cdot p)^N \times \int_0^1 dx x^{N+3-D/2} (1-x)^{4-D/2} \int_0^1 dy y^{N+2} (1-y)^{D/2-4} \int_0^1 dz z^N (1-z). \quad (3.28)$$

Here, the Feynman parameters decompose into Beta-functions, Eq. (3.17). The ε -expansion performed with MAPLE yields

$$\begin{aligned} I_1 &= a_s^2 S_\varepsilon^2 \left(\frac{m^2}{\mu^2} \right)^\varepsilon (\Delta \cdot p)^N \Gamma(N+1) \\ &\quad \times \exp(-\varepsilon \gamma_E) \frac{\Gamma(2-\varepsilon) \Gamma(N+2-\varepsilon/2) \Gamma(3-\varepsilon/2) \Gamma(-1+\varepsilon/2)}{\Gamma(N+5-\varepsilon) \Gamma(N+2+\varepsilon/2)} \\ &= a_s^2 S_\varepsilon^2 \left(\frac{m^2}{\mu^2} \right)^\varepsilon (\Delta \cdot p)^N \frac{1}{(N+1)(N+2)(N+3)(N+4)} \\ &\quad \times \left[\frac{4}{\varepsilon} + (-5 + 4S_1(N+4) - 4S_1(N+1)) + \mathcal{O}(\varepsilon) \right] \end{aligned} \quad (3.29)$$

This last expression contains single harmonic sums which are defined as

$$S_1(N) = \sum_{k=1}^N \frac{1}{k}. \quad (3.30)$$

In general one can define multiple finite harmonic sums $S_{a_1, \dots, a_n}(N)$ as [21]

$$S_{a_1, \dots, a_n}(N) = \sum_{k_1=1}^N \sum_{k_2=1}^{k_1} \dots \sum_{k_n=1}^{k_{n-1}} \frac{\text{sign}(a_1)^{k_1}}{k_1^{|a_1|}} \dots \frac{\text{sign}(a_n)^{k_n}}{k_n^{|a_n|}}. \quad (3.31)$$

The ε -expansion of Eq. (3.29) did not directly yield the result in terms of harmonic sums. Prior to this we had to use the relation [22]

$$S_k(N) = \frac{(-1)^{k-1}}{(k-1)!} \psi^{(k-1)}(N+1) + \zeta_k, \quad (3.32)$$

with $\psi^{(k)}(N)$ being the k -th derivative of the ψ -function, which is the logarithmic derivative of the Γ -function. Making use of (3.30) one can write (3.29) as a purely rational function of the

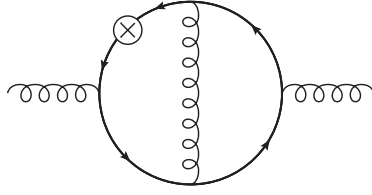


Figure 6: Two-loop diagram with external gluons.

Mellin-moment N .

$$I_1 = -a_s^2 S_\varepsilon^2 \left(\frac{m^2}{\mu^2} \right)^\varepsilon (\Delta \cdot p)^N \frac{1}{(N+1)(N+2)(N+3)(N+4)} \\ \times \left[\frac{4}{\varepsilon} - \frac{5N^3 + 33N^2 + 58N + 16}{(N+2)(N+3)(N+4)} + \mathcal{O}(\varepsilon) \right]. \quad (3.33)$$

As we saw, this first two-loop integral is of the same complexity as the one-loop integrals.

3.2.2 A Second loop-topology

Let us now study the diagram depicted in Fig. 6. The calculations for this diagram have been carried out in [14, 18, 23]. Its Feynman-parametrization will lead to a new class of functions. The analytic expression for the diagram is given by

$$I_2 = -g^4 (m^2)^2 \int \frac{d^D k}{(2\pi)^D} \frac{d^D l}{(2\pi)^D} \frac{1}{(p+k)^2 - m^2} \frac{1}{(p+l)^2 - m^2} \frac{1}{l^2 - m^2} \\ \times \frac{1}{k^2 - m^2} (\Delta \cdot k)^N \frac{1}{k^2 - m^2} \frac{1}{(l-k)^2}. \quad (3.34)$$

Also here we perform the same steps as described above and obtain an expression consisting of Feynman-parameter integrals only

$$I_2 = \frac{\Gamma(6-D)}{(4\pi)^D} (m^2)^{-4+D} \int_0^1 dx_1 dx_2 dx_3 dy_1 dy_2 dy_3 \delta(x_1 + x_2 + x_3 - 1) \delta(y_1 + y_2 + y_3 - 1) \\ [x_3(1-x_3)]^{-3+D/2} (1-y_1-y_3) y_3^{2-D/2} \left(y_1 + y_3 \frac{x_1}{(1-x_3)} \right)^N \left(1 - y_3 + \frac{y_3}{x_3} \right)^{-6+D}. \quad (3.35)$$

In contrast to the two-loop topology calculated above, the computation of the Feynman-parameter integrals is more involved. At first we integrate x_2 and y_2 using the δ -distributions since they do not appear in the integrand at other places. One has to rewrite these integrals in the following way

$$\int_0^1 dx_2 \delta(x_1 + x_2 + x_3 - 1) = \int_{-\infty}^{+\infty} dx_2 \theta(x_2) \theta(1-x_2) \delta(1-x_1-x_2-x_3), \quad (3.36)$$

where $\theta(z)$ denotes the Heaviside-function. Now the δ -functions can be integrated and the remaining θ -functions restrict the integration range of x_1 and y_1 . Performing the substitutions $x_1 = z_1(1-x_3)$ and $y_1 = z_2(1-y_3)$ and setting $x_3 = x$, $y_3 = y$ one obtains

$$I_2 = \frac{\Gamma(6-D)}{(4\pi)^D} g^4 (m^2)^{-4+D} \int_0^1 dx dy x^{-3+D/2} (1-x)^{-2+D/2} y^{2-D/2} (1-y)^2 \left(1 - y + \frac{y}{x} \right)^{-6+D} \\ \times \int_0^1 dz_1 dz_2 (1-z_2) [z_2(1-y) + z_1 y]^N. \quad (3.37)$$

The z -integrals can be solved in terms of elementary functions giving

$$I_2 = \frac{\Gamma(6-D)}{(4\pi)^D} g^4(m^2)^{-4+D} \int_0^1 dx dy x^{-3+D/2} (1-x)^{-2+D/2} y^{1-D/2} \left(1-y+\frac{y}{x}\right)^{-6+D} \\ \times \frac{1+y^N \left\{ \left(\frac{1-y}{y}\right)^N (y-1)^3 + y^2 [N(y-1) + 2y - 3] \right\}}{(N+1)(N+2)(N+3)}. \quad (3.38)$$

At this point the interesting new mathematical structures appear. The x -integration is of the form of the hypergeometric function ${}_2F_1$ [24], which has an integral representation [19]

$${}_2F_1(\alpha, \beta; \gamma; z) = \frac{1}{B(\beta, \gamma - \beta)} \int_0^1 dt t^{\beta-1} (1-t)^{\gamma-\beta-1} (1-zt)^{-\alpha}, \quad \text{Re}\gamma > \text{Re}\beta > 0. \quad (3.39)$$

We also consider analytic continuations of this function [19]. Using this relation one can solve the x -integration for this Euler-function. The remaining y -integration can be done as follows. Performing the substitution $y = 1 - z$ one obtains

$$I_2 = \frac{\Gamma(6-D)}{(4\pi)^D} g^4(m^2)^{-4+D} \int_0^1 dz B(4-D/2, -1+D/2) {}_2F_1\left(6-D, 4-D/2; 3, \frac{z}{z-1}\right) \\ \times (1-z)^{-5+D/2} \frac{1 - (1-z)^N \left\{ \left(\frac{z}{1-z}\right)^N z^3 + (1-z)^2 [Nz - 2(1-z) + 3] \right\}}{(N+1)(N+2)(N+3)}. \quad (3.40)$$

In order to integrate this expression, the argument of the ${}_2F_1$ -function has to be transformed using [19]

$${}_2F_1\left(\alpha, \beta; \gamma, \frac{z}{z-1}\right) = (1-z)^\alpha {}_2F_1(\alpha, \gamma - \beta; \gamma; z). \quad (3.41)$$

Combining Eq. (3.41) with Eq. (3.40) one can use the equality [19]

$$\int_0^1 dz z^{\mu-1} (1-z)^{\nu-1} {}_2F_1(\alpha, \beta; \gamma; z) = B(\mu, \nu) {}_3F_2(\alpha, \beta, \mu; \gamma, \mu + \nu; 1), \quad (3.42)$$

in order to obtain

$$I_2 = \frac{g^4(m^2)^{-4+D} \Gamma(6-D) B(4-D/2, -1+D/2)}{(4\pi)^D (N+1)(N+2)(N+3)} \\ \times \left[B(1, 2-D/2) {}_3F_2(6-D, -1+D/2, 1; 3, 3-D/2; 1) \right. \\ - B(N+4, 2-D/2) {}_3F_2(6-D, -1+D/2, N+4; 3, N+6-D/2; 1) \\ - NB(2, N+4-D/2) {}_3F_2(6-D, -1+D/2, 2; 3, N+6-D/2; 1) \\ + 2B(1, N+5-D/2) {}_3F_2(6-D, -1+D/2, 1; 3, N+6-D/2; 1) \\ \left. - 3B(1, N+4-D/2) {}_3F_2(6-D, -1+D/2, 1; 3, N+5-D/2; 1) \right]. \quad (3.43)$$

The function ${}_3F_2$ is a generalized hypergeometric function [24] and part of the function class ${}_pF_q$, which are well known in mathematical literature [19]. They all obey the following series representation for $|z| < 1$

$${}_pF_q(\alpha_1, \dots, \alpha_p; \beta_1, \dots, \beta_q; z) = \sum_{k=0}^{\infty} \frac{(\alpha_1)_k \cdots (\alpha_p)_k}{(\beta_1)_k \cdots (\beta_q)_k} \frac{z^k}{k!}, \quad (3.44)$$

with the Pochhammer-symbol [24]

$$(\alpha)_k = \frac{\Gamma(\alpha + k)}{\Gamma(\alpha)}. \quad (3.45)$$

The ε -expansion and the infinite summation can be done with the help of the computer algebra package SIGMA [25] giving the result

$$I_2 = a_s^2 S_\varepsilon^2 \left(\frac{m^2}{\mu^2} \right)^\varepsilon \left\{ \frac{3 + 2N + 2N^2 + N^3}{(N+1)^3(N+2)^2(N+3)} + \frac{1}{(N+1)^2(N+2)(N+3)} \left[\frac{3}{2}(N+1)S_2(N) + \frac{1}{2}(N+1)S_1^2(N) - NS_1(N) \right] \right\}. \quad (3.46)$$

The function $S_2(N)$ is a harmonic sum as defined for the general case in Eq. (3.31).

4 Summary

In this report we were dealing with the theory of deeply inelastic electron-proton scattering. In tree-level approximation of electroweak theory we identified the hadronic tensor, Eq. (1.5), to be the object of our interest. One particular part of the latter, the structure functions $F_i(N, Q^2)$, contain the full information of the nucleon structure. At certain physical limits, namely large virtualities, these functions factorize into perturbatively accessible Wilson coefficients $C_i^j(N, Q^2)$ and non-perturbative parton distribution functions $f_j(N, \mu^2)$. The Wilson coefficients contain a structure, called massive operator matrix elements $A_{ij}(N, m^2)$. These OMEs or more precisely the OME $A_{Qg}(N, m^2)$, contributing to the structure function F_2 has been calculated and renormalized to one-loop order. In order to calculate the loop integral, different techniques had to be applied: Wick-rotation, Feynman-parametrization and D -dimensional momentum integration among others. Here, the Feynman-parameter integrals could be solved in terms of well known Beta- and Γ -functions.

In addition to the one-loop calculations, the scalar parts of two two-loop topologies were investigated. Integrating loop by loop, the first of these topologies could be treated exactly in the same way as the one-loop integrals yielding the same mathematical structures. The second topology investigated was more difficult to solve. Integrating out both loop momenta the Feynman-parameter integrations could not be trivially performed. In their evaluation they revealed rich mathematical structures. The function class we obtained there is called in the literature generalized hypergeometric functions. In both topologies the ε -expansion was performed.

To put it in a nutshell, the theory of deeply inelastic scattering is an attractive playground for complex analysis. It is fascinating to see how new mathematics is generated by the evaluation of simple Feynman diagrams and even more interesting that these mathematical structures have a great application in physical theories as the theory of the strong interaction.

Acknowledgements

My special thanks goes to my supervisor Prof Dr. Johannes Blümlein for the plenitude of discussions and his extraordinary support during the summer student programme and in writing this report. Furthermore, I want to thank the group, especially Alexander Hasselhuhn, for his support and shared insights. Especially, I thank Irina Petrushina and Igor Isaev for their moral support in writing this report and during the whole summer student programme.

References

- [1] M. Gell-Mann, *Phys. Lett.* **8** (1964), 214
- [2] G. Zweig, *Preprints*, CERN-TH-412 (1964)
- [3] J. Blümlein, M. Klein, T. Naumann, T. Riemann, *Proc. of DESY Theory Workshop on Physics at HERA*, Hamburg, West Germany, Oct 12-14, ed. R.D. Peccei, PHE-88-01 (1987) 39pp
- [4] S.D. Drell, J.D. Walecka, *Annals Phys.* **28** (1964), 18
- [5] S.B. Libby, G. Sterman, *Phys. Rev.* **D18** (1978),3252,4737;
R.K. Ellis, H. Georgi, M. Machacek, H.D. Politzer, G.G. Ross, *Phys. Lett.* **B78** (1978), 281 (1978),3252,4737;
D. Amati, R. Petronzio, G. Veneziano, *Nucl. Phys.* **B140** (1978),54;
J.C. Collins, D.E. Soper, G. Sterman, *Nucl. Phys.* **B261** (1985), 104;
G.T. Bodwin, *Phys. Rev.* **D31** (1985), 2616 [Erratum-ibid. **D34** (1986), 3932]
- [6] H. Mellin, *Acta Soc. Sci. Fennica*, **21** (1896), 1; *Acta Math.* **25** (1902), 139
- [7] C.G. Bollini, J.J. Giambiagi, *Nuovo Cim.* **B12** (1972), 20; *Phys. Lett.* **B40** (1972), 566
- [8] G. t'Hooft, M.J.G. Veltman, *Nucl. Phys.* **B44** (1972), 189
- [9] J. F. Ashmore, *Nuovo Cim.* **4** (1972), 289
- [10] G.M. Cicuta, E. Montaldi, *Lett. Nuovo Cim.* **1972**, 329
- [11] F.J. Yndurain, *Quantum Chromodynamics* (Springer-Verlag, NewYork, 1983)
- [12] W.A. Bardeen, A.J. Buras, D.W. Duke, T. Muta *Phys. Rev.* **D18** (1978), 3998
- [13] G. t'Hooft, *Nucl. Phys.* **B61** (1973), 455
- [14] M. Buza, Y. Matiounine, J. Smith, R. Migneron, W.L. van Neerven, *Nucl. Phys* **B472** (1996), 611
- [15] D.J. Gross, F. Wilczek, *Phys. Rev.* **D8** (1973), 3633
- [16] D.J. Gross, F. Wilczek, *Phys. Rev.* **D9** (1974), 980
- [17] H. Georgi, H.D. Politzer, *Phys. Rev.* **D9** (1974), 416
- [18] J. Blümlein, I. Bierenbaum, S. Klein *Nucl. Phys. B* 780 (2007), 40-75
- [19] I.S. Gradstein, I.M. Ryshik, (Tables, Verlag Harri Deutsch, Frankfurt/M., 1981)
- [20] J. Blümlein, I. Bierenbaum, S. Klein, *Nucl. Phys. B* 820 (2009), 417-482
- [21] J.A.M. Vermaseren *Int. J. Mod. Phys. A* **14** (1999) 2037[hep-ph/9806280];
J.Blümlein, S. Kurth, *Phys. Rev. D* **60** (1999) 014018 [hep-ph/9810241]
- [22] J. Blümlein, *Comp. Phys. Comm.* 180 (2009), 2218-2249
- [23] J. Blümlein, I. Bierenbaum, S. Klein *Phys. Lett. B* 648 (2007), 195

- [24] L.J. Slater, *Generalized Hypergeometric Series*, (Cambridge University Press, Cambridge, 1935)
- [25] C. Schneider, *J. Symbolic Comput.* **43** (2008), 611; *Ann. Comb.* **9** (2005), 75; *J. Differ. Equations Appl.* **11** (2005), 799; *Ann. Comb.* **14** (4) (2010), [arXiv:0808.2543v1]; Proceedings of the Workshop "Motives, Quantum Field Theory, and Pseudodifferential Operators", held at the Clay Mathematics Institute, Boston University, June 2-13, 2008, Clay Mathematics Proceedings **12** (2010), 285-308, Eds. A. Carey, D. Ellwood, S. Paycha, S. Rosenberg; *Sém. Lothar. Combin.* **56** (2007), 1, Article B56b, Habilitationsschrift JKU Linz (2007) and references therein;
J. Ablinger, J. Blümlein, S. Klein, C. Schneider, *Nucl. Phys. (Proc. Suppl.)* **205-206** (2010), 110 [arXiv: 1006.4797 [math-ph]]